

Efficiency Measurement Method for UHF Transponder Antennas

Lukas W. Mayer and Arpad L. Scholtz

Vienna University of Technology

Institute of Communications and Radio-Frequency Engineering

Gusshausstrasse 25/389, 1040 Vienna, Austria

Web: <http://www.nt.tuwien.ac.at>

Email: lukas.mayer@tuwien.ac.at

Abstract—In this paper we address methods for characterizing small, low-gain antennas that are intended to be operated autonomously by a passive transponder chip. We present a way to perform accurate 3D gain measurements by means of a small, battery-powered, calibrated signal source and a two axis rotation apparatus. From the measurement results the directional pattern and the antenna efficiency are derived. We perform a test measurement of a half-wavelength dipole and find good accordance of measured and theoretical data.

I. INTRODUCTION

The performance of an RFID (radio frequency identification) transponder consisting of a transponder antenna and a transponder chip is a critical factor in the design of an RFID system. Whereas standard compliant chips are offered by a number of vendors, the antenna is usually subject to custom design and optimization because it has to deal with the given environment. With field simulation software tools available today, antenna design can be done theoretically to quite an advanced stage—however, the properties of the low-cost manufacturing process and materials can only be explored through testing of prototypes. In most cases a variety of prototypes are built and tested in a certain scenario using an interrogator [1]. To overcome the manufacturing tolerances of chip and antenna, a number of prototypes have to be tested for each design variant. Such a measurement campaign may consume a large amount of time, especially if the performance of the transponder in combination with different goods or different environments is to be explored.

To avoid uncertainties that are caused by the transponder chip and to save time, a measurement of the bare antenna without the chip can quickly and accurately reveal the antenna's input impedance, radiation pattern, and efficiency. These results also allow to quickly match the antenna to a certain chip. Measuring the antenna as it will be used in the intended application provides the designer with details about proximity effects and helps to create more reliable transponders.

In Section II we will present one way of doing a gain measurement that allows the characterization of small RFID transponder antennas in the UHF frequency band. The results make possible a fair comparison of different antenna structures. When using a special test oscillator described in Sec-

tion III, transponder antennas can be measured autonomously without the disturbance of a measurement cable. The apparatus that allows to automatically rotate the antenna around two axes is discussed in Section IV. In Section V we will present results obtained for a half-wavelength dipole that verify the measurement procedure.

II. DIRECTIONAL PATTERN AND ANTENNA EFFICIENCY MEASUREMENT

This section discusses antenna characterization methods that allow proper measurement of directional pattern, gain, and efficiency of transponder antennas.

The fact that transponder antennas have to be low cost often rules out the use of quality materials and a precision manufacturing process like etched copper. In addition to that the antennas are preferred to be small. These constraints have an impact on the antenna efficiency which is often below 30%. Furthermore, the radiation pattern of small antennas approaches that of a Hertzian dipole which means that there is no substantial directivity. When a cable is used to connect such an antenna with measurement equipment, common mode currents will be induced along the cable. These currents will much more seriously corrupt the measurement results of a low directivity antenna than observed with a highly directive antenna. A small, high-quality balun might reduce this problem if the cable extends exactly along the antenna's symmetry plane. Experiments in an anechoic chamber showed that if this is not the case, input impedance and radiation pattern measurements are not reproducible. Surrounding the cable with absorbing material reduces common mode currents which improves the accuracy of the input impedance measurement. On the other hand the absorbing material drains energy from the field which leads to inaccurate gain and efficiency figures.

Results that reveal the characteristics of the antenna when combined with a transponder chip and placed in a certain environment can thus only be achieved by a measurement that does not require a cable [2], [3]. The gain can therefore best be measured by the use of a small, autonomous calibrated receiver or transmitter that is directly connected to the transponder antenna.

In order to achieve accurate gain figures, this unit has to be

- small (ideally chip size) to maintain the performance of the antenna,
- well matched to the antenna,
- operating autonomously without cables,
- sufficiently stable over time, and
- must not radiate electromagnetic field by itself.

After careful consideration we decided to build a calibrated transmitter that complies sufficiently well with these requirements. It will be described in Section III

Once a gain measurement is set up, the directional pattern of the antenna can be determined. This is done by rotating the antenna around two axes (azimuth and elevation) with an adequate angle increment and taking a series of gain measurements. To calculate the total radiated power, both the horizontally and the vertically polarized field components have to be determined. From these results the radiated power for each polarization is calculated according to

$$P_{\text{Rad},i} = \int_0^{2\pi} \int_0^\pi P_{\text{In}} \frac{G_{\text{Iso},i}(\vartheta, \varphi)}{4\pi} \sin(\vartheta) d\vartheta d\varphi, \quad (1)$$

where $G_{\text{Iso},i}(\vartheta, \varphi)$ denotes the antenna gain for polarization i (horizontal or vertical) compared to the isotropic radiator and P_{In} denotes the power that is available at the antenna input [4]. The symbols φ and ϑ refer to the azimuth and the polar angle coordinate, respectively. Finally, the antenna efficiency can be calculated as

$$\eta = \frac{P_{\text{Rad,Hor}} + P_{\text{Rad,Ver}}}{P_{\text{In}}}.$$

III. TEST OSCILLATOR

In this section we describe the design and the electrical characteristics of a small test oscillator that complies with the requirements stated in Section II.

The transmit signal at 866 MHz is generated by a Hartley type LC-oscillator (Figure 1). The oscillator is built around an npn-bipolar transistor (2SC5080) in common base configuration. A collector current of 5 mA was chosen to generate an output power of 2 dBm in the oscillator stage. The tapped inductor L1 is an air wound coil made of 0.6 mm silvered copper wire that consists of 4+1 turns with an inner diameter of 1.5 mm and a pitch of approximately 1.2 mm. The capacitance of the winding together with the collector-base capacitance forms a parallel resonant circuit. The frequency can be tuned by compressing or expanding the inductor. Feedback is achieved by the capacitor C1.

Experiments with the oscillator powered directly by a 3V lithium button cell (CR1216, 25 mAh) showed that the signal power and frequency strongly depend on the battery status. Therefore, a low-dropout, low-noise voltage regulator (LT1964ES5-BYP) was inserted. The resistors R6 and R7 set the output voltage to 2 V. This enables stable operation of the oscillator until the battery voltage drops below 2.3 V. Figure 2 depicts the oscillator's frequency f and output power P versus time. It is seen that during the first 10 minutes of operation the frequency rises slightly. This is due to thermal effects in the oscillator transistor and in the voltage regulator.

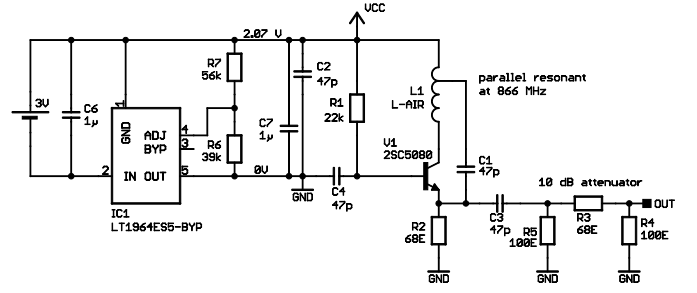


FIGURE 1 – OSCILLATOR SCHEMATIC.

Then, output power and frequency remain sufficiently constant for approximately 40 minutes—long enough to conduct the antenna measurement procedure. After 50 minutes of operation the voltage of the button cell drops below 2.3 V thus causing a decay in output power and an increase in frequency. Throughout the antenna measurements, the frequency is monitored by the receiver to detect a possible battery failure.

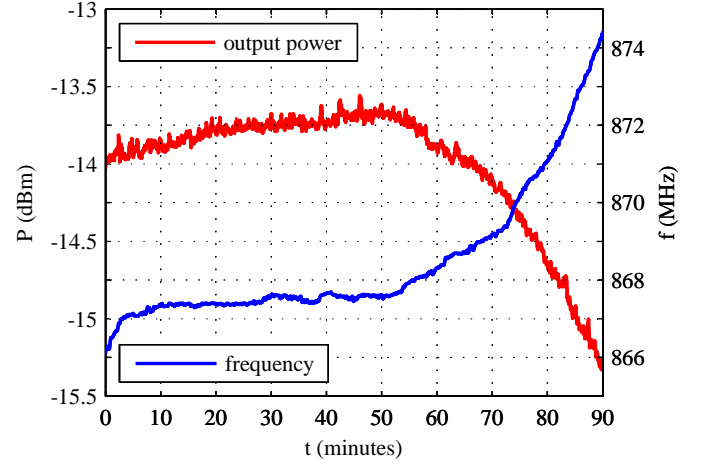


FIGURE 2 – OSCILLATOR OUTPUT POWER AND FREQUENCY VERSUS TIME.

At the output, the oscillator is equipped with a DC-blocking capacitor (C3) and a π -attenuator (R3, R4, and R5). The attenuator reduces possible interaction between the oscillator and the antenna and provides an accurate output impedance of 50Ω ($|S_{11}| < -25 \text{ dB}$). A short piece of 50Ω semi-rigid coaxial cable (UT-047) with a female mini-SMP connector at its end is soldered to the test oscillator. A surface mounted mini-SMP male connector is soldered to the antenna providing a severable, quick, and reliable connection between antenna and oscillator. Figure 3 shows a photograph of the small, battery-driven oscillator attached to the dipole antenna. The size of the oscillator is $25 \times 11 \text{ mm}^2$.

For the characterization of transponder antennas, the attenuator will be replaced by a tunable matching network consisting of trimmer capacitors and resistors. This network can be tuned to optimally match the antenna's input impedance. Matching between oscillator and antenna is identified by a maximum of radiated power. Furthermore, by successive measurement of

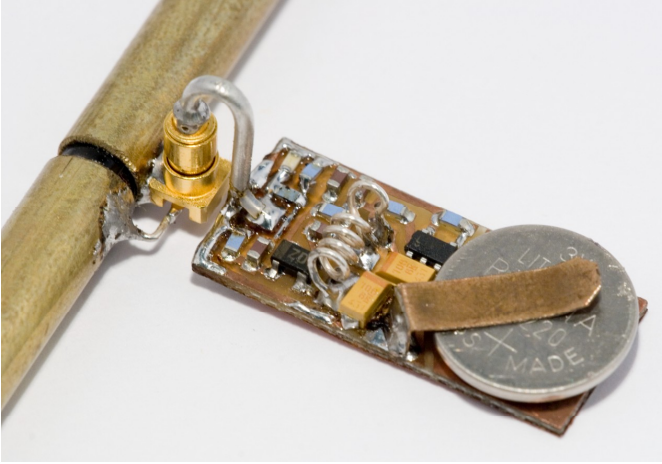


FIGURE 3 – PHOTOGRAPH OF THE BATTERY DRIVEN OSCILLATOR.

the oscillator's source impedance Z_{Osc} , the antenna impedance is found with $Z_{\text{Ant}} = Z_{\text{Osc}}^*$ (source pull measurement). The measurement error introduced by the electrical delay and capacitance of the mini-SMP connector is considered to be negligible. This method enables input impedance measurements at the transponder antenna without the use of a measurement cable.

Please note that during the test measurement (Section V), the electromagnetic field radiated by the oscillator itself (primarily produced by the coil) was more than 20 dB weaker than the field radiated by the half wavelength dipole. For conducting measurements on low-gain antennas, the oscillator will be surrounded by thin copper foil to further reduce its radiated field.

IV. ROTATION UNIT

To automate antenna pointing, an apparatus was designed that incorporates an azimuth rotator that is placed on the floor of an anechoic chamber. On top of this rotator a tower made of polystyrol foam is mounted. The height of this tower is adjustable. The transponder antenna is attached to the elevation unit that consists of a stator and a rotor also made from polystyrol foam. Stator and rotor are connected by ball bearings that consist of polyurethane rings and glass balls. Attached to the rotor, there is a disc made from Rohacell that drives the rotor via a perlon cord that is moved by a stepper motor located at the bottom of the tower. This design offers the following advantages:

- 1) No conducting elements are included in the apparatus except for the ones located at the floor of the chamber which are "hidden" by pyramid absorbers.
- 2) There are no materials that show significant dielectric constant except for the small glass balls and polyurethane rings that are contained in the bearings.

This very well preserves the natural propagation of electromagnetic waves like in free space and thus enables exploring the radiation behavior of an antenna pointing in any direction.

A photograph of the elevation unit that is located at the top of the tower is shown in Figure 4.

Please note that for the sake of simplicity of the apparatus, the dipole is mounted horizontally. This implies that the calibrated pickup antenna also has to be aligned horizontally to characterize the dipole's radiation pattern for vertical polarization. Consequently, rotating the tower axis modifies the polar angle ϑ whereas turning the rotor at the top of the apparatus modifies the azimuth angle of the dipole measurement.

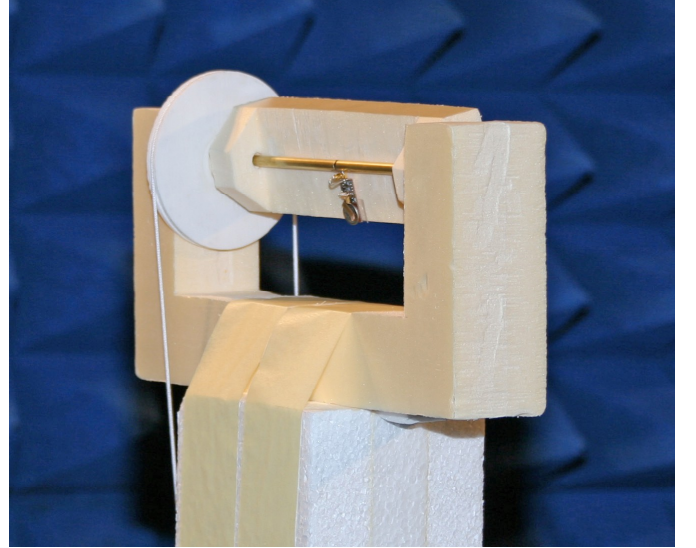


FIGURE 4 – PHOTOGRAPH OF THE ROTATION UNIT WITH THE HALF-WAVELENGTH DIPOLE AND THE TEST OSCILLATOR ATTACHED.

V. TEST MEASUREMENT

For testing, we measured a half wavelength dipole (thickness $d = 6$ mm, length $l = 147$ mm, input impedance $Z_{\text{IN}} \simeq 50 \Omega$, center frequency $f_c = 866$ MHz) in an anechoic chamber. To distinguish between horizontal and vertical polarization the calibrated receiver antenna was tilted by 90° . The transmission distance was $d = 2.88$ m and thus sufficient to be in the far field. The results for the dipole were obtained by performing the following measurement procedure:

- 1) Power up the oscillator and wait for the oscillator signal to be stable (10 minutes).
- 2) Measure the distance d between the device under test and the calibrated reference antenna.
- 3) Measure the output power $P_{\text{Out, Oscillator}}$ and the frequency f of oscillator.
- 4) Connect the oscillator to the device under test and attach the device under test to the rotation unit.
- 5) Start the automated measurement program in Matlab (angle increment $\Delta_\varphi = \pi/20$ and $\Delta_\vartheta = \pi/12$).
- 6) Flip the receiver antenna for the measurement of the other polarization and repeat Step 5.
- 7) Doublecheck the output power and the frequency of the oscillator.

- 8) Convert the received power P_{Receive} to the antenna gain G_{DUT} according to

$$G_{\text{DUT}} = \frac{P_{\text{Receive}}/G_{\text{Ref}}}{P_{\text{Out, Oscillator}}} \cdot \left(\frac{4\pi d}{c_0/f} \right)^2.$$

The measurement was carried out in a shielded anechoic chamber. A calibrated log-periodic reference antenna with a gain of $G_{\text{Ref}} = 6.2$ dBi was used. From the measured antenna gain for horizontal and vertical polarization versus azimuth and polar angle, the antenna efficiency was calculated. This was done by approximating the integrals with sums in Equation (1). Table I shows the results obtained from the measurement and the corresponding theoretical values (linear scale). It can be seen that the measurement results agree with the theoretical results for an ideal dipole by approximately one decibel. This is a typical accuracy for an antenna gain measurement with reasonable effort.

TABLE I – DIPOLE ANTENNA MEASUREMENT RESULTS

antenna parameter	value	theoretical value
efficiency	133 %	100 %
peak gain	2.05	1.64
cross polarization ratio	102.5	∞

A graphical representation of the antenna gain is given in Figure 5. The vertical gain pattern G_{Ver} agrees well with the ideal characteristic of a dipole—except for a dependence of the elevation pattern on the azimuth angle φ . In the figure this is identified as a wave-like distortion in the vertical gain pattern. Obviously, the small oscillator attached to the dipole antenna causes a slight tilt of the effective dipole axis by some few degrees. The measured gain for horizontal polarization G_{Hor} —that should be zero in theory—results from the tilt of the effective dipole axis as well. Uncertainties caused by imperfect cross polarization capabilities of the reference antenna or depolarization effects in the chamber seem to be negligible. This is confirmed by the consistent dependence of horizontal and vertical antenna gain on the azimuth angle φ . Please note that for the sake of better perception, the horizontal gain is shown with a magnification of 50 in Figure 5.

VI. CONCLUSION

In this paper we presented a method to characterize RFID transponder antennas. The critical factors in measuring small autonomous antennas without the use of a measurement cable are addressed and a solution approach comprising a small, battery powered LC-Oscillator is presented. A unit that rotates the antenna in both azimuth and elevation allows to obtain a series of gain figures from which the antenna efficiency can be calculated. The verification measurement results for a half-wavelength dipole agree well with the theoretical data.

ACKNOWLEDGEMENTS

We would like to thank DI Wolfgang Müllner, Seibersdorf Research, Electromagnetic Compatibility and RF-Engineering,

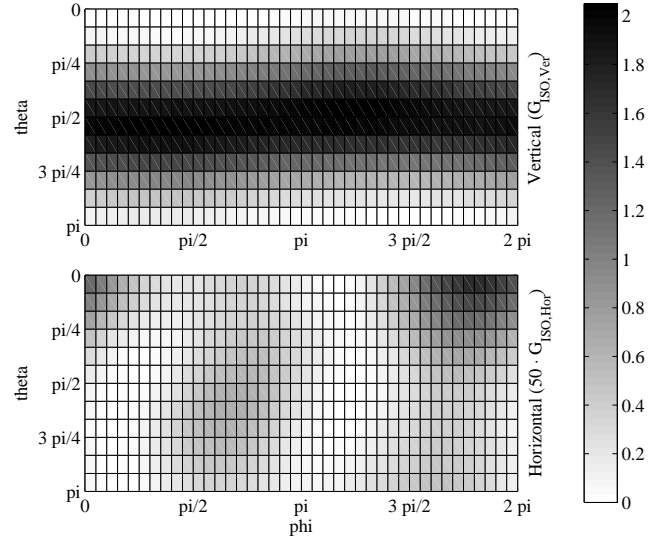


FIGURE 5 – GAIN PATTERN OF THE DIPOLE ANTENNA FOR HORIZONTAL AND VERTICAL POLARIZATION.

for valuable discussions and for granting us access to the anechoic chamber. Furthermore, we would like to thank the members of the Christian Doppler-Laboratory Christoph Angerer, Bastian Knerr, Martin Holzer, and Ayse Adalan for giving us an overview of transmission techniques and recent RFID standardization [5].

REFERENCES

- [1] P. V. Nikitin and K. V. S. Rao. Theory and measurement of backscattering from RFID tags. *IEEE Antennas Propagat. Mag.*, 48(6):212–218, Dec. 2006.
- [2] Pawel Kabacik, Arkadiusz Byndas, Robert Hossa, and Marek Bialkowski. A measurement system for determining radiation efficiency of a small antenna. In *Proceedings of the European Conference of Antennas and Propagation: EuCAP 2006*. European Space Agency, Nov. 2006.
- [3] Donald J. Gray. 3D antenna measurement system - low gain antenna measurements and CTIA OTA testing. In *Proceedings of the European Conference on Antennas and Propagation: EuCAP 2006*. European Space Agency, Nov. 2006.
- [4] Hiroyuki Arai. *Measurement of Mobile Antenna Systems*. Artech House, Inc., 685 Canton Street, Norwood, MA 02062, 2001.
- [5] C. Angerer, B. Knerr, M. Holzer, A. Adalan, and M. Rupp. Flexible simulation and prototyping for RFID designs. In *Proceedings of the EURASIP Workshop on RFID Technology*, Sept. 2007.